Int. J. Electrochem. Sci., 6 **(2011)** 5470 - 5481

International Journal of
ELECTROCHEMICAL
SCIENCE
www.electrochemsci.org

Spectroscopic and Electrochemical Studies on The Binding Mechanism of DNA With an Anthraquinone Biological Dye, Nuclear Fast Red

Qingxiang Wang [1,2,*], *Xueling Wang*[2], *Zhanglong Yu*[1], *Xianlong Yuan*[3], *and Kui Jiao*[3]

[1] Department of Chemistry and Environmental Science, Fujian Province University Key Laboratory of Analytical Science, Zhangzhou Normal University, Zhangzhou, 363000, P. R. China Zhanglong Yu
[2] Department of Chemistry and Chemical Engineering, Heze University, Heze, 274015, P. R. China
[3] College of Chemistry and Molecular Engineering, Qingdao University of Science and Technology, Qingdao, 266042, P. R. China
[*]E-mail: axiang236@126.com

Received: 11 September 2011 / *Accepted:* 15 October 2011 / *Published:* 1 November 2011

In this work, the interaction of an anthraquinone dye, nuclear fast red (NFR) with fish-sperm DNA was studied via spectrometry, viscometry and electrochemical methods. A weak hypochromic effect was observed for the characteristic absorption peaks of NFR, and its wavelengths had no shift in the presence of DNA, showing the external binding mode of NFR to DNA. The fluorescent spectra experiments showed that DNA could quench the emission spectra of NFR with a moderate Stern–Volmer quenching constant (K_{sv}) of 1.5×10^3 M^{-1}, which was also consistent with an external binding mode. DNA viscosity experimental results further suggested that NFR did not intercalate into the base pairs of DNA. Electrochemical method was also applied to study the interaction between NFR and DNA, and the binding constant (K) and binding site size (s) of NFR with DNA were determined to be 3.3×10^5 M^{-1} and 3.5, respectively, based on voltammetric titration method.

Keywords: Nuclear fast red; DNA; Binding mechanism

1. INTRODUCTION

DNA is one of the most important biomacromolecules in life processes. It plays an important role in the process of storing, copying and transmitting gene messages. DNA is also a major target for drugs and some harmful chemicals, and the studies on the binding nature of these small molecules to DNA are important and fundamental issues on life science because these drugs and chemicals can significantly influence the genetic information expression and result in some diseases related to the cell proliferation and differentiation [1-2]. Generally, the small molecules interact with DNA via three

kinds of noncovalent modes, *ie.*, (i) intercalating between stacked base pairs, (ii) noncovalent groove binding, or (iii) electrostatic bind to the negatively charged nucleic acid sugarphosphate skeleton [3]. The detailed investigation on the interaction of small molecules with DNA is helpful for us to design the highly efficient antitumor drugs [4-5] or to well understand the toxic mechanisms of harmful chemicals, such as environmental pollutants, pesticides, etc [6-7].

Anthraquinones, a kind of organic compound which was widely applied in industry and medicine, and thus the human population is frequently exposed to them. However, little information concerning their hazards to human has yet been accumulated [8], so, with the consideration of human heath, the examination on the correlation of anthraquinones and toxicity was required. Nuclear fast red (NFR, also named calcium red, Kernechtrot, *et al*. Chemical structure see Scheme 1) is a typical anthraquinone dye, and as general anthraquinones, possessing the ability to mediate a one-electron transfer to molecular oxygen to form superoxide anion radicals and to generate reactive oxygen species upon visible light illumination [9]. It was often served as the counterstain in many biological experiments [10-11]. While little attention has been paid to the biological influence of this dye, especially its binding properties with the biological macromolecules such as proteins and nucleic acid were even less. The clarification on the binding mechanism of these stains to biological macromolecules could help us to understand the biological value and toxicity of them.

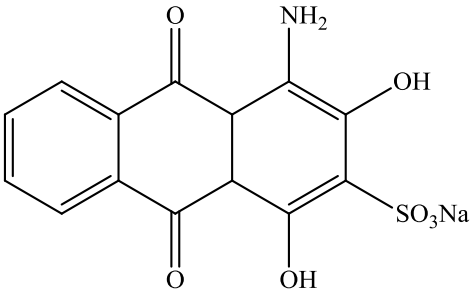

Scheme 1. Chemical structure of NFR

In this paper, the interaction of the anthraquinones dye, NFR with herring sperm DNA was carefully studied via spectrometry, viscometry and electrochemical methods. Experimental results showed that this dye interacted with DNA via a groove-binding mode. These conclusions might have potential values for further understanding the biological effect of this kind of dyes.

2. MATERIALS AND METHODS

2.1. Materials

Native fish sperm DNA from Beijing Baitai Biochemistry Technology Company (China) was used as received. The stock solution of DNA was prepared by dissolving appropriate amount of DNA in doubly distilled water and stored at 4 ºC for use. The ratio of the absorbance at 260 and 280 nm

(A_{260}/A_{280}) was checked to be ~1.89, indicating that the DNA was sufficiently free from protein. The concentration of DNA in nucleotide phosphate was determined spectrophotometrically at 260 nm using the known molar extinction coefficient value of 6600 L/mol/cm [12]. NFR was purchased from Shanghai Chemical Reagent Company of Chinese Medical Group (China). Ethidium bromide (EB) was obtained from Jiangsu Beyotime Institute of Biochemistry (China). Britton-Robinson（B-R）buffer solution war used to adjust the pH of the test solution. The other reagents purchased commercially were of analytical reagents and doubly distilled water was used throughout.

2.2. Apparatus and methods

UV-Vis experiments were carried out on a Cary 50 probe spectrophotometer (Varian, Australia). Fluorescent experiments were measured with Hitachi F-4500 fluorospectrometer (Japan) by keeping the concentration of NFR constant (1.0×10^{-5} M) while varying the DNA concentration from 0 to 1.34×10^{-3} M. The excitation wavelength was fixed at 520 mm and the emission range was adjusted before measurements. Viscosity experiments were carried out using an Ubbelodhe viscometer maintained at a constant temperature at 30±0.1 ºC in a thermostatic water-bath. Flow time was measured with a digital stopwatch and each sample was measured three times, and an average flow time was calculated. Data were presented as $(\eta/\eta_o)^{1/3}$ versus binding ratio of [NFR]/[DNA] or [EB]/[DNA], where η is the relative viscosity of DNA in the presence of NFR or EB, and η_o is the relative viscosity of DNA alone. Viscosity values were calculated from the observed flow time of DNA-containing solutions corrected for the flow time of 0.02 M pH 7.0 B-R buffer solution alone (t_0), $\eta = t - t_0$. Electrochemical assays were performed by using CHI 832 electrochemical analysis system (China) with three-electrode system consisted of a bare glassy carbon working electrode (GCE, Φ = 3 mm), a saturated calomel reference electrode (SCE), and a platinum wire auxiliary electrode. All the electrochemical measurements were carried out in a 10 mL electrochemical cell. A model pHS-25 digital acidometer (China) was used to adjust the pH value of the buffer solution.

3. RESULTS AND DISCUSSION

3.1. Electronic absorption spectra

Electronic absorption spectra were initially used to investigate the interaction between NFR and DNA. Figure 1 shows the UV spectra of NFR interaction with different concentrations of DNA. It was observed that NFR had two strong absorption peaks at 520.0 nm and 558.0 nm, respectively, with a shoulder peak at 480 nm. After interaction with increasing amount of DNA, all the peaks decreased gradually and the wavelength had no obvious shift. Long et al. [3] had pointed out that the absorption peaks shift of the small molecules after they interacted with DNA could be as the clues to judge the binding mode between the small molecules and DNA: If the binding involves a typical intercalative mode, an hypochromism effect coupled with obviouse bathochromism for the characteristic peaks of the small molecules will be found due to the strong stacking between the chromophore and the base

pairs of DNA. Therefore, based on this viewpoint, the interaction way between NFR and DNA could be noncovalent groove binding. This conclusion was also consistent with the other groove binders reported in the literatures [13-14].

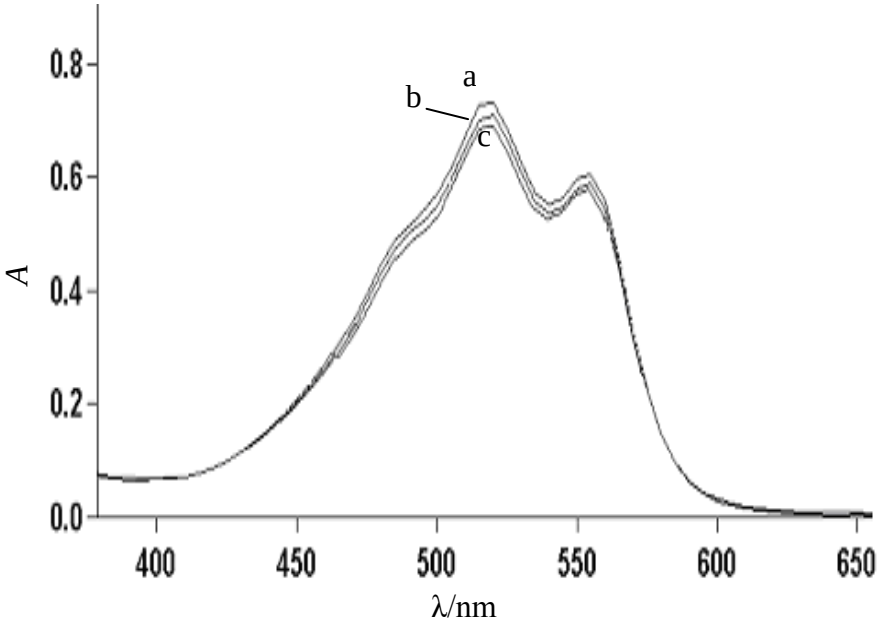

Figure 1. Electronic absorption spectra of 5×10^{-5} M NFR interaction with 0 (a), 1.7×10^{-4} M (b), 3.4×10^{-4} M (c) DNA in 0.04 M pH 4.0 B-R buffer

3.2. Fluorescent spectra

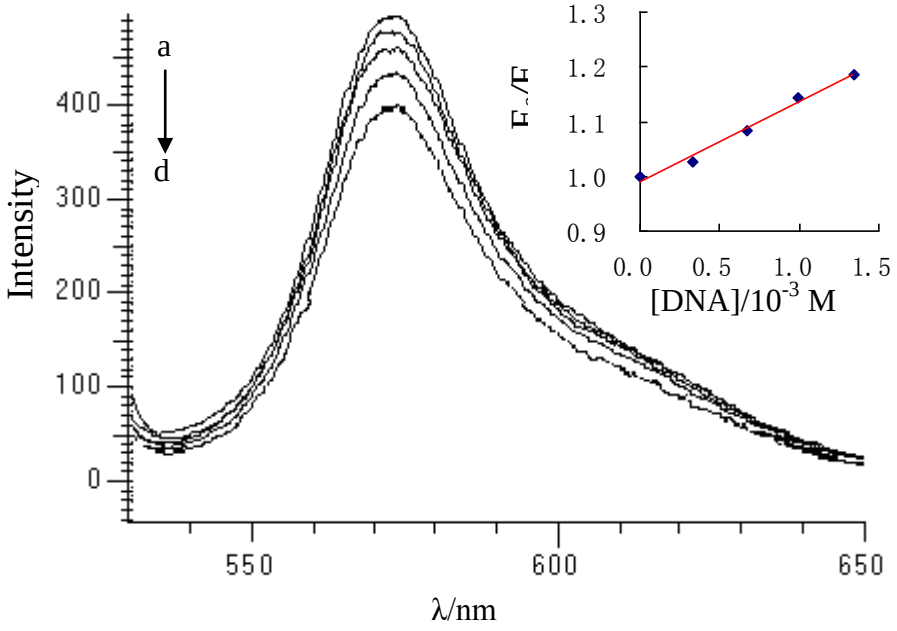

Figure 2. Fluorescence spectra of 10 μM NFR in the absence (a) and presence of 0.33 (b), 0.67 (c), 1.00 (c) and 1.34 (d) mM DNA in 20 mM pH 4.0 B-R buffer

The interaction of NFR with DNA was also studied via fluorescent spectra, and the results were showed in Figure 2. It could be clearly observed that NFR showed an obvious emission peak at 574 nm. After adding different concentration of DNA into the NFR solution, the fluorescence intensity of NFR was found to be quenched obviously under the same conditions, which could be assigned to the photoinduced electron-transfer reaction between the excited NFR and the nucleic bases [15]. Additionally, it has been reported that there are two quenching types in characterizing the binding mechanism of quencher and macromolecules: static and dynamic (or collision) quenching. Static quenching refers to the formation of a non-fluorescence fluorophore–quencher complex, and the dynamic quenching refers to the quencher diffused to the fluorophore during the lifetime of the exited state upon contact, the fluorophore returns to ground state without emission of a photon [16]. The mechanism of the dye binding to DNA could be probed using the following Stern–Volmer equation [17].

$$\frac{F_0}{F} = 1 + K_{SV}[DNA] \quad (1)$$

Where F_0 and F are the fluorescence intensities in the absence and presence of DNA, respectively, [DNA] is the DNA concentration, K_{sv} is the Stern–Volmer quenching constant, which can be considered as a measure for efficiency of fluorescence quenching by DNA. For the studied interaction system, the Stern–Volmer plot was given in inset of Figure 2. The typical linear relationship of F_0/F versus [DNA] suggested that the quenching effect for this system was a static type, *i. e.*, a non-fluorescence complex was formed between NFR and DNA. Additionally, the Stern–Volmer quenching constant, K_{sv} obtained from the plots was determined to be 1.5×10^3 M^{-1} (five points), which was obviously lower than the other classical intercalators like nile blue (3.2×10^6 M^{-1}) [18] and 2-tert-butyl-4-methylphenol (1.3×10^4 M^{-1}) [19] showing the relatively lower affinity of the studied anthraquinone dye than the other intercalators, which was also in agreement with the binding strength difference between the groove-binding and the intercalation [20].

3.3. Viscometry

For further clarifying on the interaction between the NFR and DNA, viscometry was carried out. As well known, optical photophysical probes are necessary, but not sufficient clues to support a binding mode between DNA and small molecules. Hydrodynamic measurement (*i.e.*, viscosity and sedimentation), which are sensitive to the length change are regarded as the least ambiguous and the most critical tests of binding mode in solution in the absence of crystallographic structural data [21]. The electrostatic binding generally has not obvious effect on the viscosity of DNA, while, a classical intercalation will result in lengthening the DNA helix as base pairs are separated to accommodate the foreign molecules, leading to the increase of DNA viscosity [22-23]. The effects of the NFR and a typical intercalator, EB on the viscosities of DNA are shown in Figure 3. For EB (Figure 3, curve a), with increasing the concentrations ratio of EB to DNA, the relative viscosities of DNA increased

gradually, which was in accordance with the previous study [24] and demonstrated the characteristic of intercalative mode.

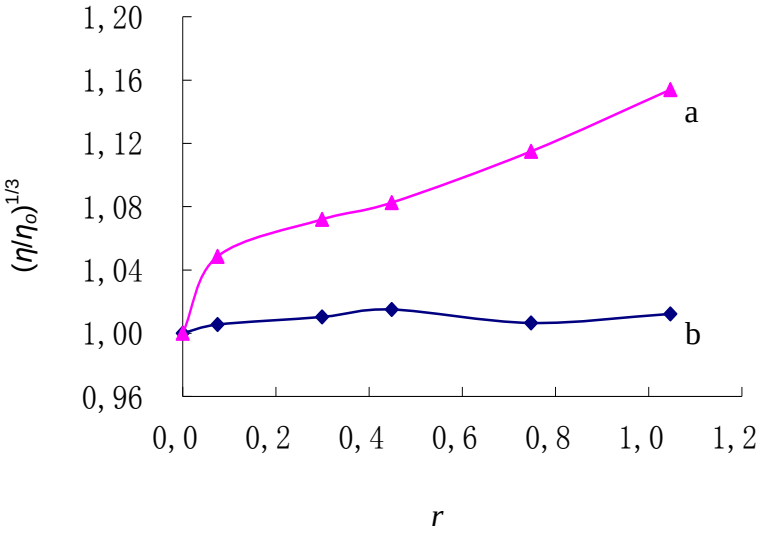

Figure 3. Effects of increasing amounts of EB (a) and NFR (b) on the relative viscosities of DNA at 30±0.1 ºC. *r* = [NFR]/[DNA] or [EB]/[DNA], [DNA]=66.9 μM.

However, for the studied dye of NFR, the relative viscosities of DNA showed little changes upon adding increasing amount of NFR (Figure 3 curve b), further accurately revealing the groove-binding mode of NFR with DNA.

3.4. Electrochemical studies

Figure 4 shows the CVs of 1.0×10^{-4} M NFR interaction with DNA in 0.02 M pH 4.0 B-R buffer solution. As showed in Figure 4 curve a, NFR has a pair of asymmetric redox peaks at -0.67 V and -0.61 V, respectively on a glassy carbon electrode surface. The ratio of the reduction peak current (I_{pc}) to oxidation peak current (I_{pa}) was much larger than one unit, suggesting that the electrochemical process of NFR at GCE was irreversible. As the reduction peak was more sensitive than the oxidation peak, so the reduction peak was chosen for further studies.

For an irreversible reduction process, the number of electron transfer (n) could be obtained by Eq. (2) [25]:

$$|E_{pc} - E_{pc/2}|=1.857RT/\alpha nF \qquad (2)$$

Where E_{pc} is the reduction peak potential, $E_{pc/2}$ the half peak potential, α the electron transfer coefficient (generally, $0.3<\alpha<0.7$), F Faraday constant (96487 coulombs/mol), R universal gas constant (8.314 J/K/mol), T Kelvin temperature. In the present study, the value of $|E_{pc}-E_{pc/2}|$=50 mV, thus the

value of n was calculated to be 1.9 (≈ 2) when α was assumed to be 0.5 for an irreversible process, suggesting that the electrochemical redution of NFR was a $2e^-$ transfer process.

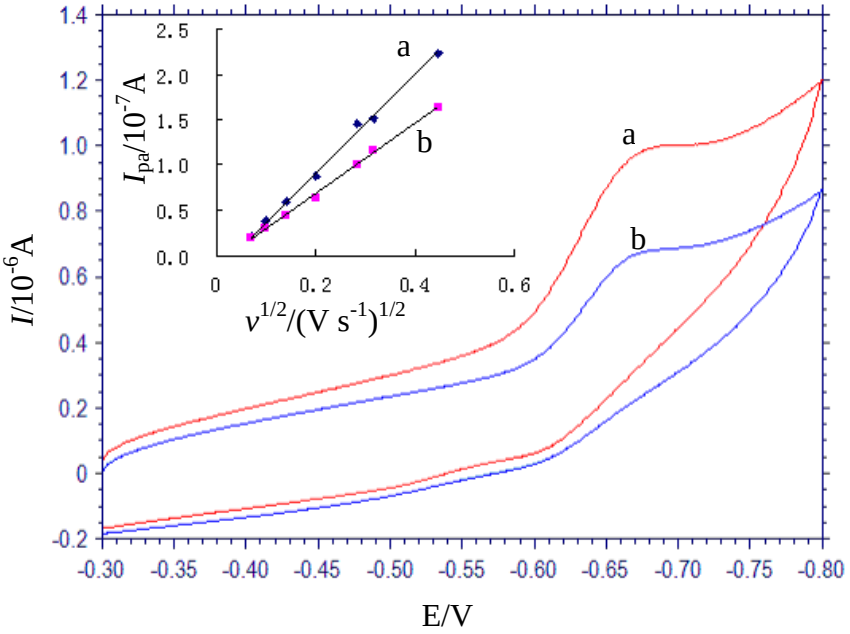

Figure 4. Cyclic voltammograms of 1.0×10^{-4} M NFR interaction without (a) and with 3.4×10^{-4} M dsDNA (b) in 0.04 M of pH 4.0 B-R. Inset: plots of I_{pc} with $v^{1/2}$ for NFR (a) and NFR -DNA complex (b)

When 3.4×10^{-4} M DNA was added into NFR solution and then voltammetrically detected under the same conditions, it was found that the reduction peak current decreased obviously accompanied by a positive shift of the reduction peak potential (Figure 4 curve b). This suggested that a new complex was formed between NFR and DNA, and the changes of the electrochemical signals after interaction with DNA were consistent with the characteristic of intercalation [26].

In a similar way, according to the value of $|E_{pc}-E_{pc/2}|$ in Figure 4 curve b and Eq. (2), the number of electron transferred was also determined to be about 2, suggesting that NFR-DNA complex also underwent a two electron transfer process.

The effects of scan rate (v) on the electrochemical signals, such as the reduction peak currents and reduction peak potentials (E_{pc}), were further studied to assess the interaction of NFR with DNA. It was well found that with increase of scan rate, the CV curves of NFR varied regularly whether DNA was present or not. Meanwhile, the plots of redution peak currents (I_{pc}) versus the square root of scan rate ($v^{1/2}$) had good linear relationships for both NFR and NFR–DNA system (inset of Figure 4), suggested that the electrochemical processes of NFR and NFR–DNA complex were both controlled by diffusion [25]. The slop of I_{pa} vs. $v^{1/2}$ for NFR-DNA complex was much smaller than that for free NFR, indicating that NFR-DNA complex diffused more slowly compared with free NFR. From this result, the decrease of peak currents of NFR upon DNA addition could be assigned to the diffusion of an equilibrium mixture of free and DNA-bound NFR to the electrode surface [25].

The changes of electron-transfer rate constants (K_s) of electroactive molecules after interaction with DNA have often been used to probe the difference of electrochemical properties between small molecules and their DNA-bound complex DNA [27,28].

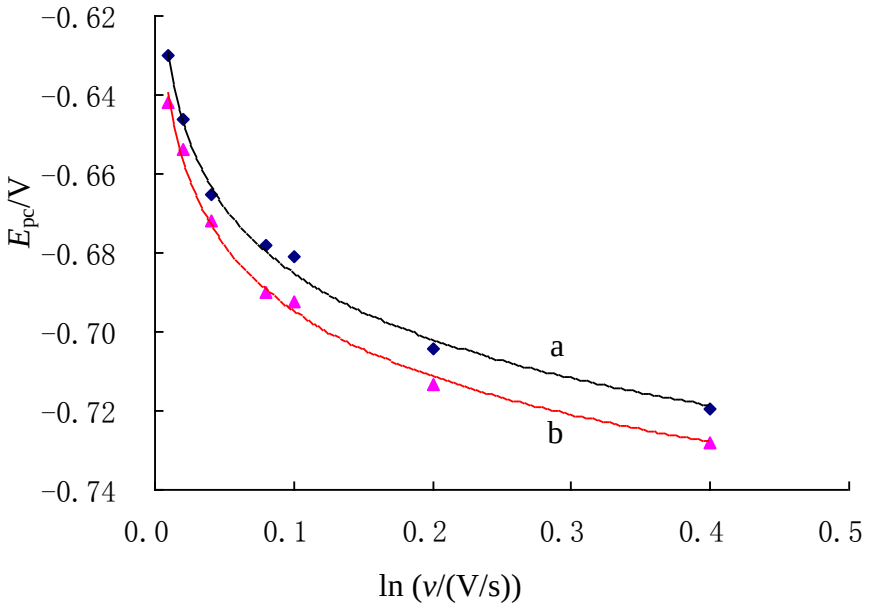

Figure 5. Relationships between the reduction peak potentials (E_{pc}) with the scan rate (v) for NFR (a) and NFR-DNA complex (b). The other conditions were the same with Figure 3.

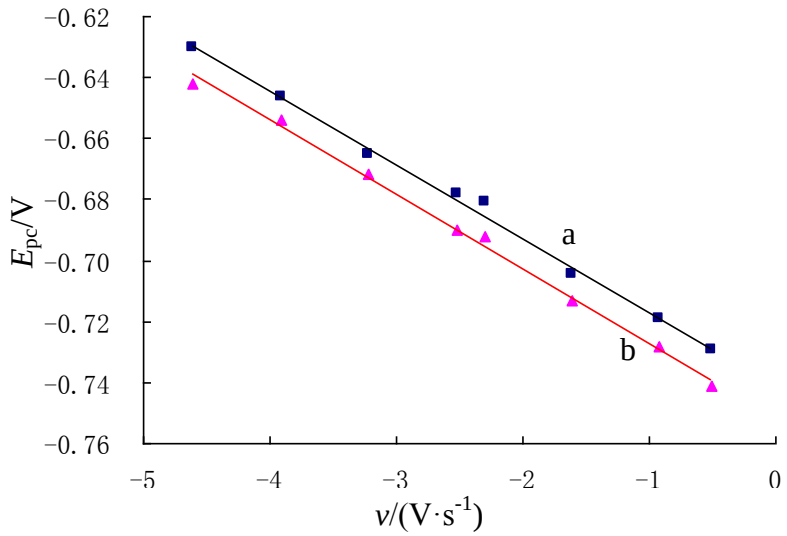

Figure 6. Relationships between the reduction peak potentials (E_{pc}) and ln v. The other conditions were the same as in Figure 3.

The plots of the reduction peak potentials (E_{pc}) of NFR (curve a) and DNA-NFR complex (curve b) with scan rate (v) were showed in Figure 5. It was well found that the peak potentials values

increased with the rising of scan rate for both of the systems. The formal potentials ($E_{pc}^{0'}$) of free and DNA-bound NFR were obtained to be -0.613 V and -0.627 V, respectively, via prolonging the $E_{pc} \sim v$ curves to *y* axis. Meanwhile, it was observed that the reduction peak potentials have good linear relationship with the logarithm of scan rate (ln *v*) for both free and DNA bound systems as showed in Fig. 6.

Thus, for an irreversible redox process, the K_s values were calculated to be 0.15 s^{-1} and 0.14 s^{-1}, respectively for free and DNA-bound NFR according to the linear relationships of $E_{pc} \sim \ln v$ and the following Laviron's Eq. (3) [29]:

$$E_{pc} = E_{pc}^{0'} + (RT/\alpha nF) \ln(\alpha nF/RTK_s) + (RT/\alpha nF)\ln v \qquad (3)$$

That was to say, after interaction with DNA, the standard rate constant, K_s of NFR-DNA almost didn't change relative to that of the free NFR. This also, from another hand, proved that the decrease of oxidation peak current of NFR after interaction with DNA was not due to the change of electron transfer kinetics, but by the decrease of the diffusion kinetics as discussed above.

Figure 7 was the DPVs of 1.0×10^{-4} M NFR in the absence (curve a) and presence of 1.1×10^{-5} M DNA (curve b). It was observed that, the oxidation peak currents of NFR decreased significantly and the peak potential was shift from -0.590 V to -0.585 V after interaction with DNA. From literature [26], it is obtained that if both the oxidized and reduced forms of a small molecule interacted with DNA, the corresponding equilibrium constants for each oxidation state binding to DNA could be calculated according to the following Eq. (4):

$$\Delta E^0 = E_b^{0'} - E_f^{0'} = (RT/nF)\ln(K_R/K_O) \qquad (4)$$

Where $E_b^{0'}$ and $E_f^{0'}$ are the formal potentials of DNA-bound and free NFR, respectively, which were determined by the formula of $E^{0'} = E_{pa} + \Delta E_p/2$, ($E_{pa}$, the DPV peak potential; ΔE_p, the pulse amplitude); K_O and K_R are the binding constants of oxidized and reduced forms to DNA, respectively.

In this work, according to the potential shift of +5 mV, the ratio of the binding constants (K_R/K_O) is calculated to be 1.5, indicating that the reduced form of NFR (NFR_{Red}) bound to DNA as strongly as 1.5 times of the oxidation form (NFR_{ox}). This result was also consistent with the characteristic of an intercalation mode [26].

The binding constant (*K*) and binding site size (*s*) were determined by voltammetric titration. The main panel of Figure 8 shows the relationship between the reduction peak currents (I_{pc}) with the concentration of DNA. It was well found that in the incipient stage, the reduction peak current decreased rapidly with the increase of DNA concentration, and then became placid when [DNA] was larger than 3.3×10^{-5} M, suggesting a complete interaction of DNA with 1.0×10^{-4} M NFR. From the inflection point (I.P.) of the titration curve, the stoichiometric point of the interaction was calculated to be 2.7×10^{-5} M. So, the binding ratio of the NFR and DNA could be determined to be 3.5, *i. e.*, one nucleotide bound with 3.5 NFR molecules on average. Further, the binding constant (*K*) of NFR with DNA was obtained by using the following equation [30]:

$$I_p^2 = \frac{1}{K[\mathrm{DNA}]}(I_{po}^2 - I_p^2) + I_{po}^2 - [\mathrm{DNA}] \qquad (5)$$

Where I_p and I_{po} are the peak currents of NFR with and without DNA, respectively.

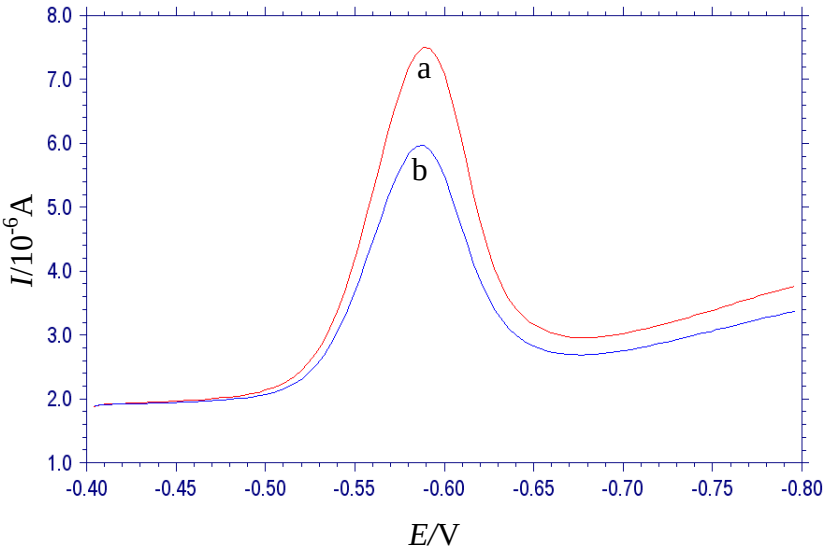

Figure 7. Differential pulse voltammograms of 1.0×10^{-4} M NFR in absence (a) and presence of 1.1×10^{-5} M DNA (b) in 0.04 M of pH 4.0 B-R buffer

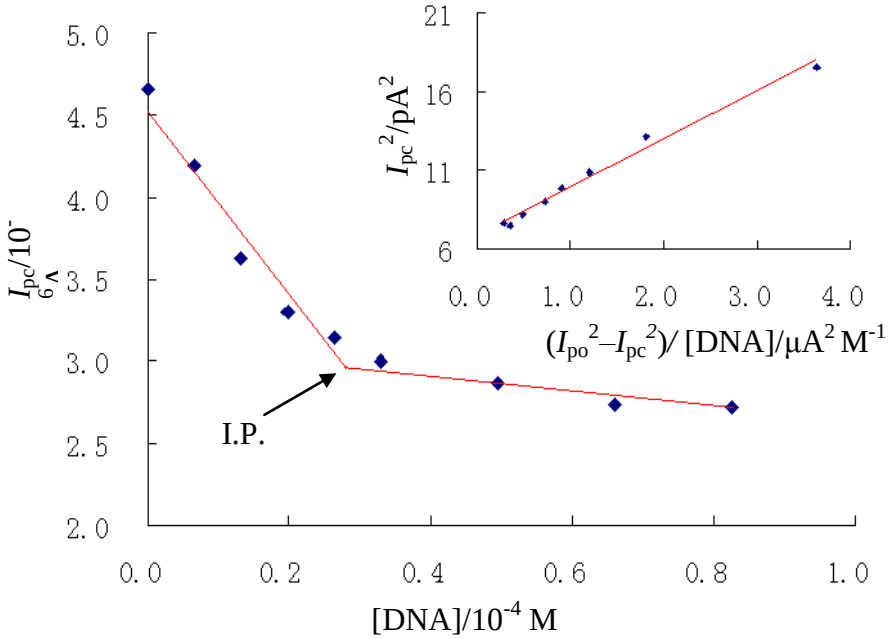

Figure 8. Plot of I_{pc}^2 vs. $(I_{po}^2 - I_{pc}^2)$/[DNA] for 1.0×10^{-4} M NFR with varying concentration of DNA in a buffer solution of 0.04 M pH 4.0 B-R.

A value of 3.3 $\times 10^5$ M^{-1} for K was then obtained from the slope of I_p^2 vs $I_{po}^2 - I_p^2$/ [DNA] plot as shown in inset of Fig. 8. The standard Gibbs free energy change ($\Delta G^0 = -RT \ln K$) comes out to be approximately -25.8 kJ/mol at 25 ℃, which indicated the spontaneity of the binding of NFR with DNA.

4. CONCLUSIONS

In this paper, the interaction of a kind of typical anthraquinone dye, NFR with DNA was comprehensively studied by spectrometry, viscometry and electrochemical methods. The obvious hypochromic effect in absorption spectra and quenching effect in fluorescent spectra of NFR in the presence of DNA initially suggested a groove binding mode between NFR and DNA, which was testified by a non-contentious viscosity experiment. Electrochemical experiments showed that NFR-DNA complex and free NFR has similar electrochemical parameters such as the electron-transferred number and electron-transferred constants. Also, the binding constant (K) and binding site size (s) of NFR with DNA were determined to be 3.3 $\times 10^5$ M^{-1} and 3.5, respectively, via voltammetric titration method.

ACKNOWLEDGMENTS

The work is supported by the National Natural Science Foundation of China (No. 20805041), Training Programme Foundation for Excellent Youth Researching Talents of Fujian's Universities (No. JA10201), Research Foundation of Fujian Education Department (No. JA11166) and Innovation Base Foundation for Graduate Students Education of Fujian Province.

References

1. X.H. Zhang, L.Y. Wang, Z.X. Nan, S.H. Tan and Z.X. Zhang, *Dyes and Pigments*, 79 (2008) 205.
2. K.L. Reddy, K.R.Y. Harish, K.K. Ashwini and S.S.S. Vidhisha, *Nucleos. Nucleot. Nucl.*, 28 (2009) 204.
3. E.C. Long and J.K. Barton , *Chem. Res.*, 23 (1990) 271.
4. T. Deligeorgiev, A. Vasilev, T. Tsvetkova and K.H. Drexhage, *Dyes and Pigments*, 75 (2007) 658.
5. K. Zhang, W. Liu, *Int. J. Electrochem. Sci.*, 6 (2011) 1669.
6. H. Shen, X. Shao, H. Xu, J. Li, S. Pan, Int. *J. Electrochem. Sci.*, 6 (2011) 532.
7. H. Shen, H. Zheng, N. Zhu, Y. Liu, J. Gao, J. Li, *Int. J. Electrochem. Sci.*, 5 (2010) 1587.
8. S. Oikawa, *Gene. Envir.*, 30 (2008) 1.
9. C. McCullagh and P.K.J. Robertson, *Photochem. Photobiol.*, 82 (2006) 1662.
10. A.G. Chiesa-Vottero, A. Malpica, M.T. Deavers, R. Broaddus, G.J. Nuovo and E.G. Silva, *Int. J. Gyn. Pathol.*, 26 (2007) 328.
11. P.L. Chen, D.J. Riley, Y. Chen and W.H. Lee, *Gene. Dev.*, 10 (1996)1870.
12. M.E. Reichman, S.A. Rice, C.A. Thomas and P. Doty, *J. Am. Chem. Soc.*, 76 (1954) 3047.
13. H.Y. Shen, Y.Q. Liu, J. Gao, H.M. Zhen, N. Zhu and J. Li, *DNA Cell. Biol.*, 30 (2011) 255.
14. S. Kashanian, M.M. Khodaei and P. Pakravan, *DNA Cell. Biol.*, 29 (2010) 639.
15. C. Bohne, K. Faulhaber, B. Giese, A. Häfner, A. Hofmann, H. Ihmels, A.K. KÖhler, S. Perä, F. Schneider and M.A.L. Sheepwash, *J. Am. Chem. Soc.*, 126 (2005) 76.
16. L. Stryer, *J. Mol. Biol.*, 13 (1965) 482.

17. J.R. Lakowicz, *Principles of Fluorescence Spectroscopy* (Kluwer Academic/Plenum, 1999 New York).
18. Q. Chen, D. Li, H. Yang, Q. Zhu, J. Xu and Y. Zhao, *Analyst*, 124 (1999) 901.
19. S. Kashanian and J.E.N. Dolatabad, *Eur. Food. Res. Technol.*, 230 (2010) 821.
20. K. Maruyama, Y. Mishima, K. Minagawa and J. Motonaka, *Anal. Chem.*, 74 (2002) 3698.
21. S. Satyanarayana, J.C. Dabrowiak and J.B. Chaires, *Biochemistry*., 31 (1992) 9319.
22. S. Satyanarayana, J.C. Dabrowiak and J.B. Chaires, *Biochemistry*, 32 (1993) 2573.
23. Y. Wang, G.W. Lin, J. Hong, T. Lu, L. Li, N. Okabe and M. Odoko, *Inorg. Chim. Acta*, 362 (2009) 377.
24. F.Q. Liu, Q.X. Wang, K. Jiao, F.F. Jian, G.Y. Liu and R.X. Li, *Inorg. Chim. Acta*, 359 (2006) 1524.
25. A.J. Bard and L.R. Faulkner, *Fundamentals and Applications* (Wilky, 1980 New York).
26. M.T. Carter, M. Rodriguez and A.J. Bard, *J. Am. Chem. Soc.*, 111 (1989) 8901.
27. F.Gao, Q. Wang, , M. Zheng, S. Li, G. Chen, K. Jiao, F. Gao, *Int. J. Electrochem. Sci.*, 6 (2011) 1508.
28. Q.X. Wang, K. Jiao, F.Q. Liu, X.L. Yuan and W. Sun, *J. Biochem. Bioph. Methods*, 70 (2007) 427.
29. E. Laviron, *J. Electroanal. Chem.*, 101 (1979) 19.
30. J. Niu, G. Cheng and S. Dong, *Electrochim. Acta*, 39 (1994) 2455.

© 2011 by ESG (www.electrochemsci.org)